NATIONAL ADVISORY COMMITTEE FOR AERONAUTICS

TECHNICAL NOTE 3426

AN EXPERIMENTAL STUDY OF ORIFICE COEFFICIENTS, INTERNAL STRUT PRESSURES, AND LOADS ON A SMALL OLEO-PNEUMATIC SHOCK STRUT

By James H. Walls

Langley Aeronautical Laboratory
Langley Field, Va.

Washington
April 1955

NATIONAL ADVISORY COMMITTEE FOR AERONAUT

TECHNICAL NOTE 3426

AN EXPERIMENTAL STUDY OF ORIFICE COEFFICIENTS, INTERNAL STRUT PRESSURES, AND LOADS ON A SMALL OLEO-PNEUMATIC SHOCK STRUT

By James H. Walls

SUMMARY

Measurements of shock-strut internal pressures, telescoping velocity, and strut stroke were made during drop tests of a small oleo-pneumatic landing gear to determine the characteristics of the orifice and to show the relationships between internal strut pressures and the overall loads developed by the strut. The range of shock-strut telescoping velocity available from the test data was between 1 and 7 feet per second and corresponded to a Reynolds number range of 9,500 to 66,500. The strut strokes available ranged between 1 and 7 inches and corresponded to approach-chamber lengths of 6.58 to 0.58 inches. Analysis of the data shows that variations in telescoping velocity and strut stroke result in relatively small changes in the orifice coefficient. Comparisons between strut forces determined from internal-pressure measurements and forces measured by an external dynamometer indicate that the strut forces can be accurately determined from the internal pressures times the appropriate areas. Comparison between time histories of strut force from internal-pressure measurements and force time histories from measurements of the telescoping velocity and strut stroke indicate that a close approximation of the strut forces during impact can be obtained when the orifice coefficient is assumed to be constant and the air-compression process to be isothermal.

INTRODUCTION

The primary function of the orifice in a landing-gear strut is to produce large dissipative forces in the shock absorber. Therefore, knowledge of the variations of orifice coefficient is desirable in shock-absorber design to permit more accurate prediction of landing-gear behavior. Although much experimental work has been done to calibrate orifices as commercial flow meters, no data were found for the type of flow conditions which exist in an oleo-pneumatic shock strut during impact. Since considerable emphasis is being given to the accurate prediction of landing-gear behavior, this paper presents the results of an investigation to

determine the characteristics of an orifice in a landing gear under the dynamic conditions present during landings. Also considered are the relationships between internal strut pressures and the overall loads developed by the strut.

SYMBOLS

A_a	pneumatic area, sq in.
A_h	hydraulic area, sq in.
A_o	area of opening in orifice plate, sq in.
C_d	orifice discharge coefficient
F_a	pneumatic force in shock strut, lb
F_h	hydraulic force in shock strut, lb
F_s	total axial shock-strut force, lb
l	approach-chamber length, in.
n	polytropic exponent for air-compression process in strut
p_a	air pressure in upper chamber of shock strut, lb/sq in.
p_h	hydraulic pressure in lower chamber of shock strut, lb/sq in.
Δp	pressure drop across the orifice, $p_h - p_a$, lb/sq in.
R	Reynolds number based on diameter of orifice and fluid velocity through that diameter
ρ	fluid density of hydraulic fluid, slugs/cu ft
s	strut stroke, in.
v_o	air volume for fully extended strut, cu in.

V_t telescoping velocity, ft/sec

V_{v_0} vertical velocity at ground contact, ft/sec

Subscript:

0 at instant of initial contact

APPARATUS

Equipment

The basic piece of equipment used in this investigation was the Langley impact-basin carriage (ref. 1) which provided means for effecting the descent of the test specimen under controlled conditions. A description of this equipment and its adaptation to the testing of landing gears is given in reference 2. During these tests the carriage was restrained in the horizontal direction and used in much the same way as a conventional landing-gear drop-testing machine.

Test Specimen

The landing gear tested was originally designed for use as a main gear on a small single-engine military training airplane having a gross weight of approximately 5,000 pounds. The shock strut and axle were connected by means of a specially designed leg incorporating an axle dynamometer, described in reference 3, which was used to obtain force measurements. The wheel was fitted with a 27-inch smooth-contour tire which was inflated to normal operation pressure of 32 pounds per square inch. The weight of the landing gear, including wheel, tire, and dynamometer, was 295 pounds. The minimum dropping weight was approximately 1,000 pounds.

The strut tested was modified in that the metering pin and snubber valve were removed and the original orifice was replaced by a smaller orifice. The orifice details and the internal arrangement of the strut are shown in figure 1 and the dimensions pertinent to this investigation are shown on the schematic representation of the shock strut presented in figure 2. The orifice plate is made of S.A.E. X4130 steel, smoothly ground and threaded to the bronze piston of the perforated supporting tube which forms the inner chamber. The strut was filled with hydraulic fluid (specification AN-VV-O-366B) through a filler plug located at the top of the strut. The kinematic viscosity of the hydraulic fluid used

in the tests was determined to be 22 centistokes or 2.365×10^{-4} ft^2/sec. Air pressure for inflating the strut was supplied through a valve located at the top of the strut. The compression ratio, which is defined as the ratio of the air volume when the strut is fully extended to the air volume when the strut is in the static position, was 4.92. The landing gear as it was mounted and instrumented for testing is shown in figure 3.

INSTRUMENTATION

A variety of time-history instrumentation was used during the tests. Pressure gages of the electrical-strain-gage type were used to measure pressure at two locations in the upper chamber (above orifice plate) and two locations in the lower chamber (below orifice plate). As shown in figure 1, pressures on the approach face of the orifice plate and on the downstream side of the orifice plate in the outer annular chamber were transmitted to the pressure gages by means of two Inconel tubes extending from the top of the strut. These pressure taps on the approach and downstream faces of the orifice plate were exposed to the pressure in the lower and upper chambers of the strut and are referred to in the following sections as low-orifice and up-orifice pressure taps, respectively. Additional measurements of the upper- and lower-chamber pressures were made by means of a pressure gage screwed into the filler-plug hole and a pressure gage screwed into the hole that originally held the metering pin. The pressure taps in the filler-plug hole and in the metering-pin hole (fig. 2) are referred to as up-oleo and low-oleo pressure taps, respectively.

The strut stroke was measured by means of a variable-resistance slide-wire potentiometer. A drag-cup generator which was positively actuated was used to measure the telescoping velocity. Measurements of the axial forces transmitted from the axle to the shock strut were obtained by means of an electrical-strain-gage-type axle dynamometer. (See ref. 3.) Since the axle dynamometer measured the forces at the axle, which differ from the forces in the shock strut by an amount equal to the inertia reaction of the mass between the shock strut and the axle, the actual shock-strut loads were obtained by subtracting the inertia reaction of the total unsprung weight less the weight of the tire and wheel assembly from the load measured by the axle dynamometer. This inertia reaction was calculated from acceleration measurements obtained from an accelerometer mounted on the landing-gear fork.

The response of the transducers together with the galvanometers was in excess of that required for this investigation. The instruments used are believed to be accurate within the following limits:

Strut stroke, in.	±0.08
Telescoping velocity, ft/sec	±0.10
Pressure, lb/sq in.	±20
Maximum vertical force from dynamometer and acceleration measurements, lb	±214

TEST PROCEDURE

The data employed in this investigation were obtained during a general landing-gear drop-test investigation carried out in the Langley impact basin. In order to minimize internal shock-strut friction and binding due to bending moments, the landing gear was attached so that the shock strut was vertical and no drag loads were simulated. Several series of drops were made with dropping weights ranging from 1,000 to 2,500 pounds and simulated wing lift ranging from free fall to almost twice the static dropping weight. The contact velocities ranged from 0 to 12 feet per second. The strut was inflated with sufficient air pressure to produce a static strut clearance between the bearing nut (item (15), fig. 1) and the landing-gear yoke (item (24)) of $1\frac{1}{2}$ inches. These conditions resulted in telescoping velocities and strut strokes which ranged up to about 7 feet per second and 7 inches, respectively.

RESULTS AND DISCUSSION

In the past, orifice investigations have been conducted almost exclusively for the purpose of calibrating orifices for the measurement of rate of flow in pipes. For such purposes the rate of flow can be readily calibrated against the difference in pressure at any two standardized locations in the pipe. The purpose of testing an orifice in a landing-gear shock strut, on the other hand, is to determine the magnitude of the damping force produced by the orifice installation under various conditions of telescoping velocity and strut stroke. Orifice coefficients which are derived from measurements of the average instantaneous pressures that govern the operation of the shock strut are, in effect, force coefficients useful in calculating the behavior of landing gears during impact. Therefore, consideration was given to the selection of pressure taps which would provide the pressures most representative of the pressures which produce the overall loads on the strut under given conditions of stroke and velocity.

Selection of Pressure Taps

From consideration of the pressures acting in the shock strut it can be seen from figure 2 that, if the friction forces between the telescoping cylinders are neglected, the total shock-strut force can be expressed in terms of the average internal strut pressures by the equation (see ref. 4)

$$F_s = p_a A_a + (p_h - p_a) A_h \qquad (1)$$

where the first term on the right-hand side represents the pneumatic or air-compression force and the second term represents the hydraulic force.

In the type of shock strut under consideration it is the pneumatic pressure in the outer annular chamber (item ⑦, fig. 1) which actually contributes to the air-compression force, because the pneumatic pressure in other parts of the strut only produce internal stresses which do not contribute to the overall strut force. In view of the fact that it was desired to evaluate the necessity of measuring the outer annular chamber pressure when a much more convenient pneumatic pressure-tap location existed (filler-plug hole which vents into inner chamber), pressures in both the outer annular and inner chambers were measured. In the hydraulic-force term in equation (1), p_h is simply the lower-chamber pressure. Since in studies of orifices in pipes it is usual to measure the approach stream pressure adjacent to the approach face of the orifice plate, the oil pressure p_h was measured at the low-orifice installation shown in figures 1 and 2. In addition to the low-orifice installation, pressure in the lower chamber was measured at the end plate (item ㉑, fig. 1) because it was convenient to do so (since a hole for the metering pin already existed) and also would provide a second pressure measurement which could be used if local fluctuations in pressure, not representative of the overall load-producing pressures, were found to exist at the low-orifice pressure-tap location.

Figure 4 shows typical time-history variations of the pressures measured at the four pressure-tap locations. Total-force curves computed by substituting these pressure measurements into equation (1) are also shown in figure 4 for the four combinations of upper- and lower-chamber pressure-tap locations. It is readily seen from this figure that the force time histories thus obtained were in reasonably good agreement regardless of the pressure-tap combination used even though there were appreciable differences between the up-oleo and up-orifice pressure measurements. This agreement between the force time histories was due mainly to the agreement between the two hydraulic pressures (low orifice and low oleo) since the pneumatic pressure contributed only slightly to the total force on the gear up to and including the time of maximum landing-gear load. An irregular rise of the up-oleo pressure was evident in all the impacts and the indicated pressure was found to deviate greatly from

the polytropic law of air compression. Since the up-oleo tap was located inside the piston-supporting tube, the irregular pressure rise recorded may be due to the dynamic pressure of the fluid jet impinging on the pressure tap. Although the up-oleo pressure measurements could satisfactorily be used in landing-gear-force calculations, the irregularities in this pressure made the up-oleo measurements unacceptable for orifice-coefficient calculations because of the dependence of the orifice coefficient upon the pressure drop $p_h - p_a$ across the orifice. Thus, the up-orifice pressure measurements (pressure in outer annular chamber) were used to represent the upper-chamber pressure for the remainder of the investigation and the low-oleo pressure was arbitrarily chosen to represent the lower-chamber pressures.

Evaluation of Landing-Gear Loads From Internal-Pressure Measurements

An evaluation of landing-gear load determined from the pressure measurements can be obtained from figure 5 which shows comparisons of landing-gear-load time histories calculated from internal-pressure measurements with corresponding load time histories of the shock-strut axial force as determined from the axle dynamometer and acceleration measurements. The forces calculated from the dynamometer measurements include friction, whereas those calculated from the pressure measurements do not. It is seen in figure 5 that, in general, the characteristics of the time histories computed by using pressure measurements were in good agreement with those obtained from the other instrumentation. If the landing gear had been inclined instead of vertical or if drag loads on the wheel had been present, the friction between the sliding surfaces of the shock strut would have been much greater and the values of shock-strut force obtained from the axle-dynamometer measurements would probably have been considerably larger in all cases than the values obtained from the pressure measurements.

On the basis of this and several similar comparisons, it is evident that the hydraulic and pneumatic pressure measurements selected provided a good representation of the pressures which produce the major portion of the landing-gear load.

Orifice Coefficients

Reduction of data and presentation of results.- In order to study the variations of pressure drop Δp and orifice discharge coefficient C_d with telescoping velocity and strut-stroke or approach-chamber length, data were obtained from approximately 30 landing impacts. The time histories

from these impacts were read at equal time increments and provided approximately 800 sets of instantaneous values of Δp, V_t, and s. By fairing and cross-plotting these data, values of Δp and V_t were obtained at constant values of s between 1 and 7 inches in increments of 1 inch. The values of Δp and V_t at constant strokes were then substituted into the following equation for the orifice coefficient C_d (see ref. 4):

$$C_d = \frac{V_t}{\sqrt{\frac{2\Delta p}{\rho}\left(\frac{A_o}{A_h}\right)^2}} \qquad (2)$$

and the resulting experimental values of C_d are represented by symbols in figure 6. In order to obtain a fairing representative of the whole mass of the data, the normal equations for linear multiple correlation (ref. 5) were used with the 800 points and the following empirical relationship between C_d, V_t, and s was obtained:

$$C_d = 0.0076V_t - 0.0041s + 0.8759 \qquad (3)$$

Equation (3) evaluated at constant values of stroke is shown by the curves in figure 6. This empirical relationship was also evaluated for constant values of telescoping velocity to obtain variations of C_d with strut stroke and the results are presented in figure 7(a). The curves of figure 6 are reproduced in figure 7(b). The scale of Reynolds number R furnished in figures 6 and 7(b) is based upon the minimum cross section of the orifice and the fluid velocity through that section.

Variation of C_d with V_t and s.- Equation (2) is based upon the commonly used assumption that, everything else being equal, the pressure drop is proportional to the velocity squared, in which case the orifice coefficient is independent of the velocity. In view of the fact that the orifice coefficient increases slightly with increasing velocity, as can be seen from figures 6 and 7 and also from equation (3), it appears that the pressure drop is not exactly proportional to the velocity squared, but rather varies as the velocity raised to some power slightly less than 2. In the tests the pressure drop actually varied as the velocity raised to about the 1.96 power. From equation (3) it is seen that the effect of velocity on the value of C_d for a given stroke amounted to less than 1 percent for each 1-foot-per-second change of V_t or approximately a 5-percent change over the range of velocity covered during these tests. It is seen from the curves of figure 7 and also from equation (3) that

the variations in strut stroke produced even smaller changes in C_d than did the variation of telescoping velocity.

In order to show the extent to which existing orifice data obtained under steady-state conditions can be used for the shock strut, a comparison is made in figure 8 of the results of the present tests and data obtained by other experimenters (refs. 6 to 8) using sharp-edge orifices, rounded-approach orifices, and venturi tubes tested in long pipes. Since the ratio of the orifice diameter to the diameter of the approach chamber (lower chamber) is 0.109 for the shock strut, comparisons are made with results of tests employing orifices and venturi tubes having small diameter ratios. The curve for the sharp-edge orifice represents data obtained for a diameter ratio of 0.2; the rounded-approach orifice, a diameter ratio of 0.182. The venturi curve is an average curve drawn through data obtained from venturi tubes of various diameter ratios ranging between 0.5 and 0.33. The orifice-coefficient data obtained from the landing-gear drop tests are shown in a band which covers the range of approach-chamber length from 0.58 to 6.58 inches.

Evaluation of Landing-Gear Loads From Orifice Coefficients

When the orifice coefficients obtained during these tests were examined at constant values of telescoping velocity and constant values of strut stroke it became apparent that the effect of variations of these two parameters on the orifice coefficient was rather small. The results thus suggest that a fairly close approximation of the hydraulic force F_h might be obtained when the orifice coefficient is assumed to have a constant value throughout the impact. By solving equation (2) for the pressure drop across the orifice and multiplying by the hydraulic area A_h, the following expression for the hydraulic force was obtained:

$$F_h = \frac{\rho A_h^3}{2\left(C_d A_o\right)^2} V_t^2 \qquad (4)$$

Equation (4) provided a means of calculating force time histories of the hydraulic force during impact from instantaneous values of V_t. For such calculation an average value of C_d equal to 0.89 was picked from the experimental data.

Figure 9 shows several comparisons of hydraulic-force time histories calculated by using experimental values of V_t in equation (4) with

hydraulic-force time histories obtained from measured instantaneous values of the internal strut pressures. The data presented in figure 9 were obtained from a typical series of free-fall drops covering a range of velocity at ground contact of 1 to 12 feet per second. It is seen from the agreement between the force calculated by the use of a constant orifice coefficient and the force from pressure measurements that the assumption of a constant value of C_d does not lead to appreciable error in reproducing the experimental variations of hydraulic force obtained during these tests.

Figure 4 shows that the pneumatic pressure contributed a relatively small amount to the total force on the landing gear during most of the impact. Nevertheless, it seemed worth while to examine the closeness with which the forces due to internal pressure could be calculated from V_t and s measurements. The pneumatic force is determined by the initial strut inflation pressure, the area subjected to the air pressure, and the instantaneous volume ratio in accordance with the polytropic law for compression of gases. Because the instantaneous air volume is equal to the difference between the initial air volume v_0 and the product of the stroke and pneumatic area A_a, the force due to the air pressure in the upper chamber can be written as

$$F_a = p_{a_0} A_a \left(\frac{v_0}{v_0 - A_a s} \right)^n \tag{5}$$

If the friction forces are neglected, the total axial force on the landing gear can be written from equations (4) and (5) as follows:

$$F_s = \frac{\rho A_h^3}{2\left(C_d A_o\right)^2} V_t^2 + p_{a_0} A_a \left(\frac{v_0}{v_0 - A_a s} \right)^n \tag{6}$$

Reference 4 shows that this is the equation that actually governs the behavior of practical landing gears. In evaluating equation (6), C_d was again given the constant value of 0.89 and, since the air-compression process is essentially isothermal (see ref. 9), the exponent n was assigned a value of 1.0.

Figure 10 shows a comparison of total landing-gear-force time histories calculated by substituting experimental instantaneous values of V_t and s into equation (6) with total landing-gear-force time histories computed by substituting into equation (1) the corresponding measured values of the internal strut pressures, which were previously shown to be in good agreement with the forces determined from the dynamometer and accelerometer measurements. The data for figure 10 were obtained from the same

series of drops that were used for figure 9. It is seen from figure 10 that the total-force time histories computed by using equations (1) and (6) are in reasonably good agreement except during the last part of the impacts where the pneumatic force contributes the major portion of the total force.

It is believed that the slight disagreement between the results during the later stages of the impact is due mainly to the fact that the value of the initial air volume v_0 used in the calculations was smaller than the actual initial air volume of the strut during the tests. The value of v_0 used in the calculations was based on the strut's being completely full of hydraulic fluid when fully compressed. In the tests, however, it appears likely that some air was trapped within the strut and prevented complete filling of the strut with fluid. Also, the loss of even a small amount of fluid when checking the strut inflation pressure or bleeding the pressure-transmitting tubes would cause appreciable error in the computed instantaneous air volume, and thus the computed pneumatic force, at the high values of stroke.

In this investigation, where the landing gear was mounted vertically and there were no drag loads on the wheel, the landing-gear loads computed from internal-pressure measurements and approximated from velocity and stroke measurements are considered to be good representations of the total force on the gear. For the cases where larger friction forces would be present it would, of course, be necessary to have data regarding the variation of the friction force during impact before the total forces on the landing gear could be accurately determined by such means.

CONCLUSIONS

Drop tests of a small oleo-pneumatic landing gear were made in the Langley impact basin. The purpose of these tests was to investigate the characteristics of an orifice in a landing gear under the dynamic conditions present during impact and to show the relation between internal strut pressures and the overall loads developed by the strut. The range of shock-strut telescoping velocity available from the test data was between 1 and 7 feet per second and corresponded to a Reynolds number range of 9,500 to 66,500. The strut strokes available ranged between 1 and 7 inches and corresponded to approach-chamber lengths of 6.58 to 0.58 inches. From time-history measurements of internal strut pressure, telescoping velocity, strut stroke, and dynamometer loads, the following conclusions are indicated:

1. For the range of Reynolds number covered during the present tests, the orifice coefficient for any particular stroke increased slightly with increasing velocity or Reynolds number. This effect, however, was small.

2. The approach-chamber length appears to have only a relatively small effect on the magnitude of the orifice coefficient. For any particular telescoping velocity the orifice coefficient decreased slightly as the strut stroke increased or as the length of the approach chamber decreased.

3. Forces calculated from measurements of internal pressure agreed with forces computed from dynamometer and accelerometer measurements.

4. A close approximation of the strut force during impact can be obtained from time-history measurements of the telescoping velocity and strut stroke when an appropriate constant average value of the orifice coefficient is chosen (in the present case, the orifice coefficient is equal to 0.89) and the air-compression process in the strut is assumed to be isothermal.

Langley Aeronautical Laboratory,
National Advisory Committee for Aeronautics,
Langley Field, Va., January 10, 1955.

REFERENCES

1. Batterson, Sidney A.: The NACA Impact Basin and Water Landing Tests of a Float Model at Various Velocities and Weights. NACA Rep. 795, 1944. (Supersedes NACA WR L-163.)

2. Milwitzky, Benjamin, and Lindquist, Dean C.: Evaluation of the Reduced-Mass Method of Representing Wing-Lift Effects in Free-Fall Drop Tests of Landing Gears. NACA TN 2400, 1951.

3. Milwitzky, Benjamin, Lindquist, Dean C., and Potter, Dexter M.: An Experimental Investigation of Wheel Spin-Up Drag Loads. NACA TN 3246, 1954. (Supersedes NACA RM L53E06b.)

4. Milwitzky, Benjamin, and Cook, Francis E.: Analysis of Landing-Gear Behavior. NACA Rep. 1154, 1953. (Supersedes NACA TN 2755.)

5. Croxton, Frederick E., and Cowden, Dudley J.: Applied General Statistics. Prentice-Hall, Inc., 1946, p. 757.

6. Tuve, G. L., and Sprenkle, R. E.: Orifice Discharge Coefficients for Viscous Liquids. Instruments, vol. 6, no. 11, Nov. 1933, pp. 201-206.

7. Smith, J. F. Downie: Calibration of Rounded-Approach Orifices. Trans. A.S.M.E., vol. 56, no. 10, Oct. 1934, pp. 791-793.

8. Anon.: Fluid Meters - Their Theory and Application. Pt. 1. Fourth ed., A.S.M.E., 1937, p. 56.

9. Walls, James H.: Investigation of the Air-Compression Process During Drop Tests of an Oleo-Pneumatic Landing Gear. NACA TN 2477, 1951.

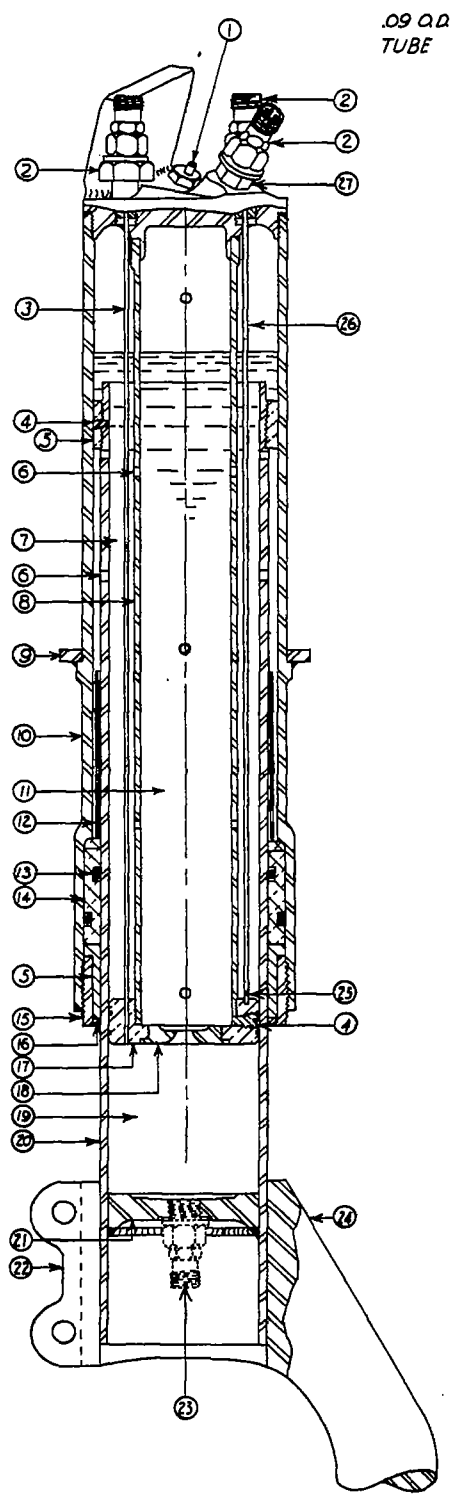

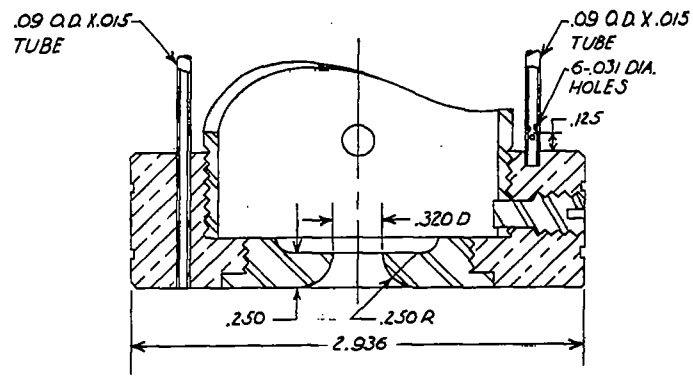

Orifice details

① Air valve
② Pressure gage
③ Low-orifice-pressure tube
④ Lock screw
⑤ Bronze bearing
⑥ Metering hole
⑦ Outer annular chamber
⑧ Piston-supporting tube
⑨ Fitting assembly flange
⑩ Outer cylinder
⑪ Inner chamber
⑫ Shock-strut spacer
⑬ Packing rings
⑭ Packing-ring spacer
⑮ Bearing nut
⑯ Wiper ring
⑰ Piston
⑱ Orifice plate
⑲ Lower chamber
⑳ Inner cylinder
㉑ End plate
㉒ Yoke collar
㉓ Lower-chamber pressure gage
㉔ Yoke
㉕ Up-orifice pressure tap
㉖ Up-orifice-pressure tube
㉗ Filler-plug location

Figure 1.- Cross section of landing-gear strut tested in Langley impact basin.

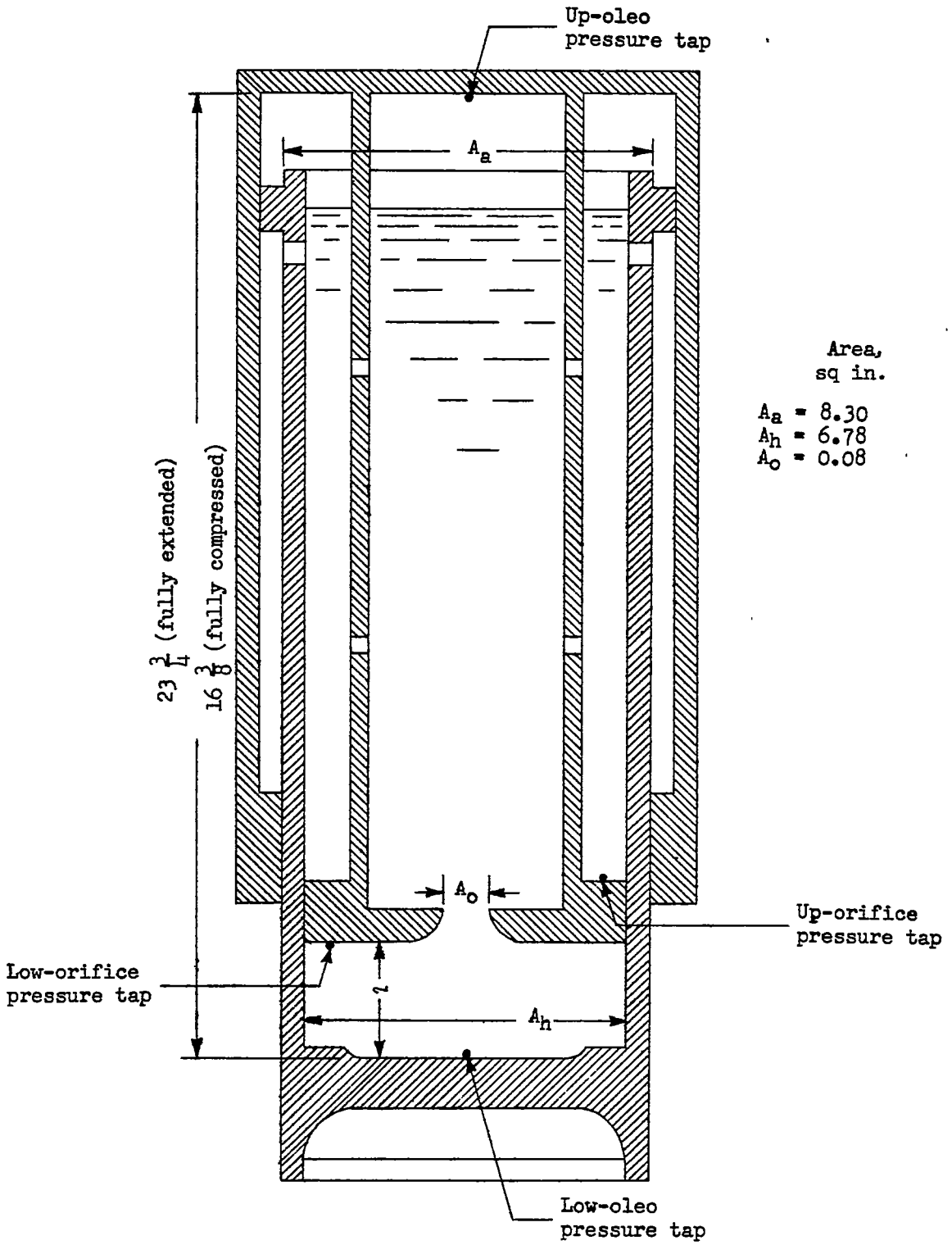

Figure 2.- Schematic representation of shock strut.

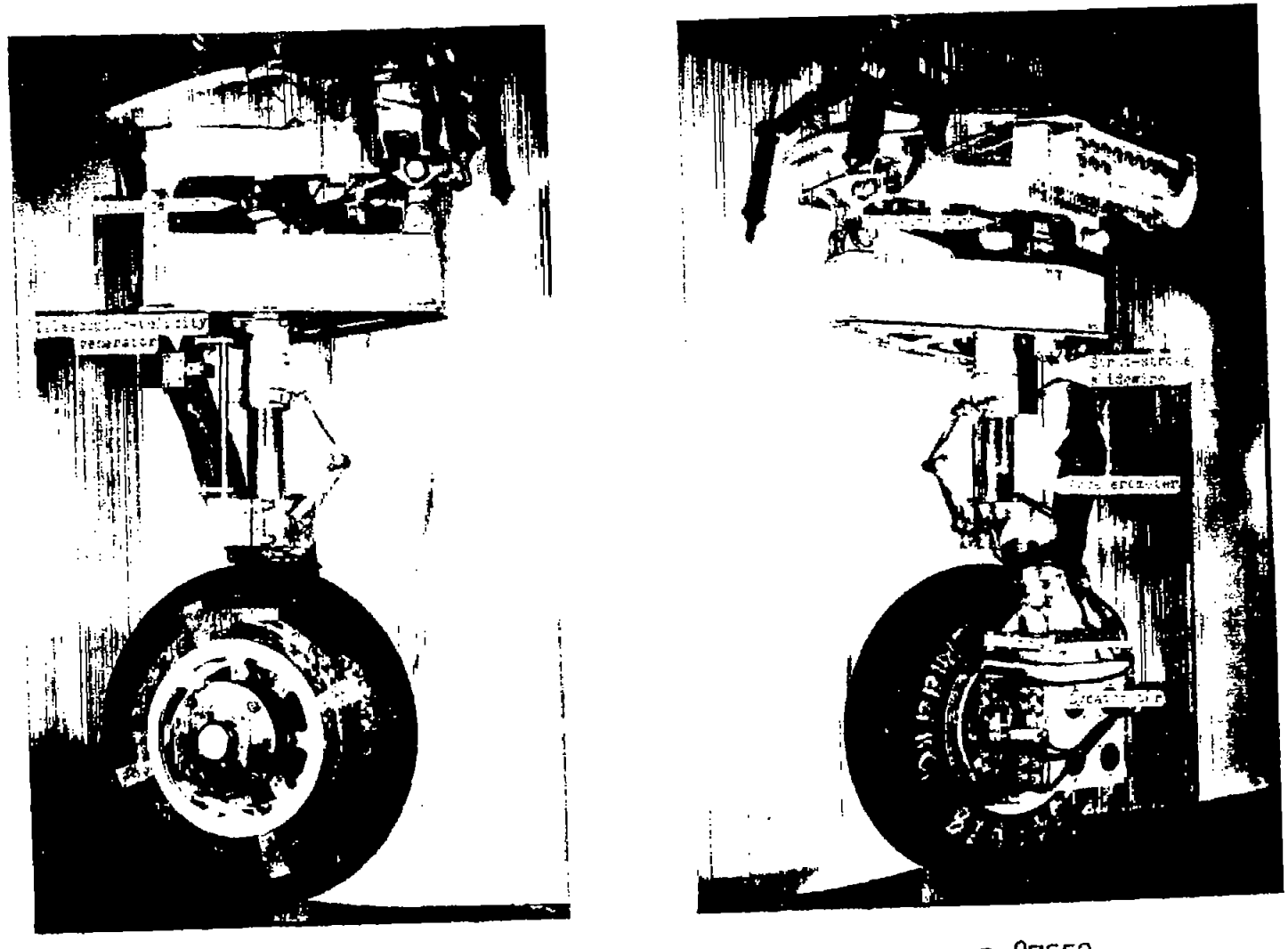

L-87552

Figure 3.- View of landing gear and instrumentation.

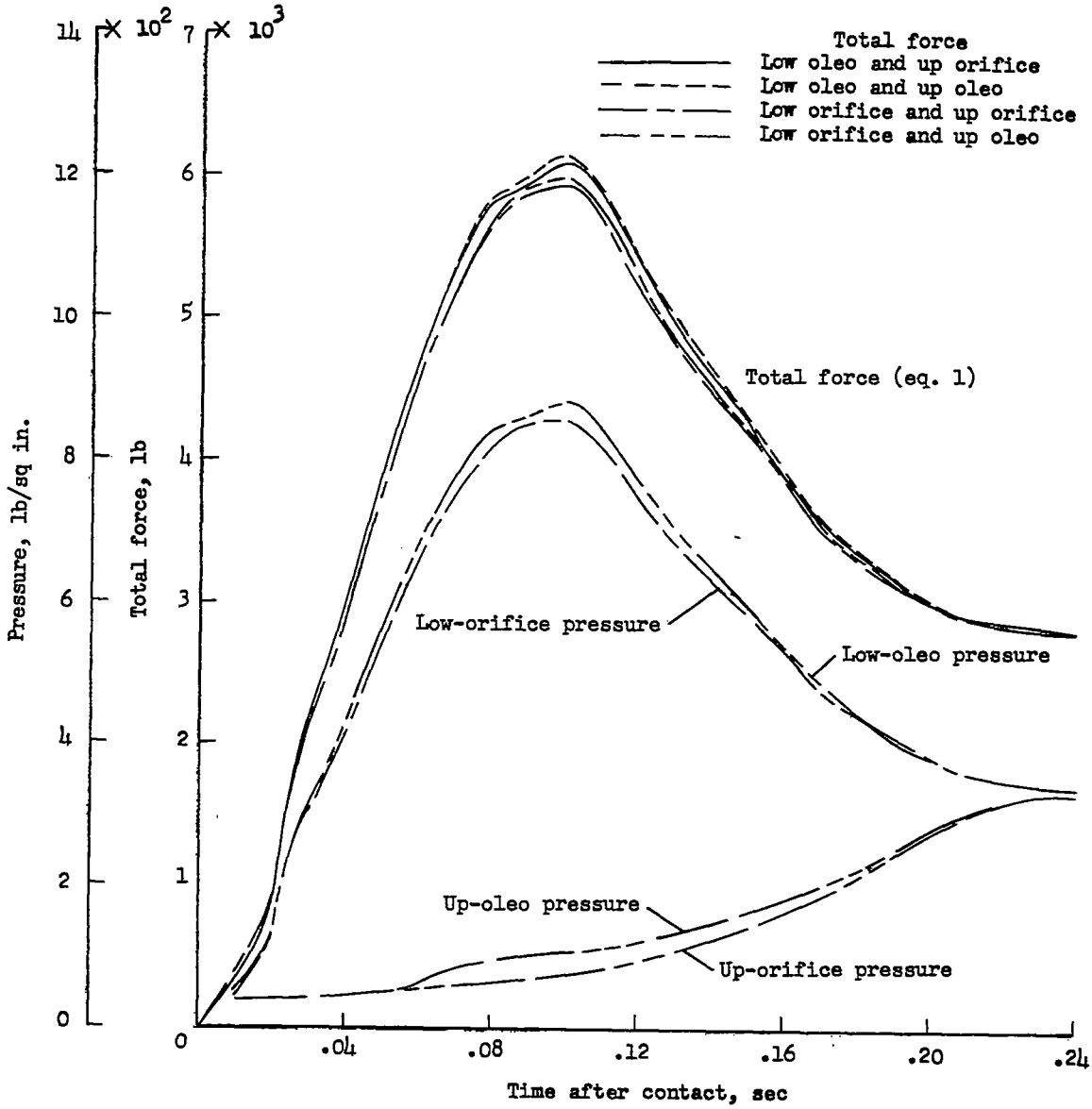

Figure 4.- Typical comparison of internal strut pressures and pressure forces determined with two different sets of pressure taps.

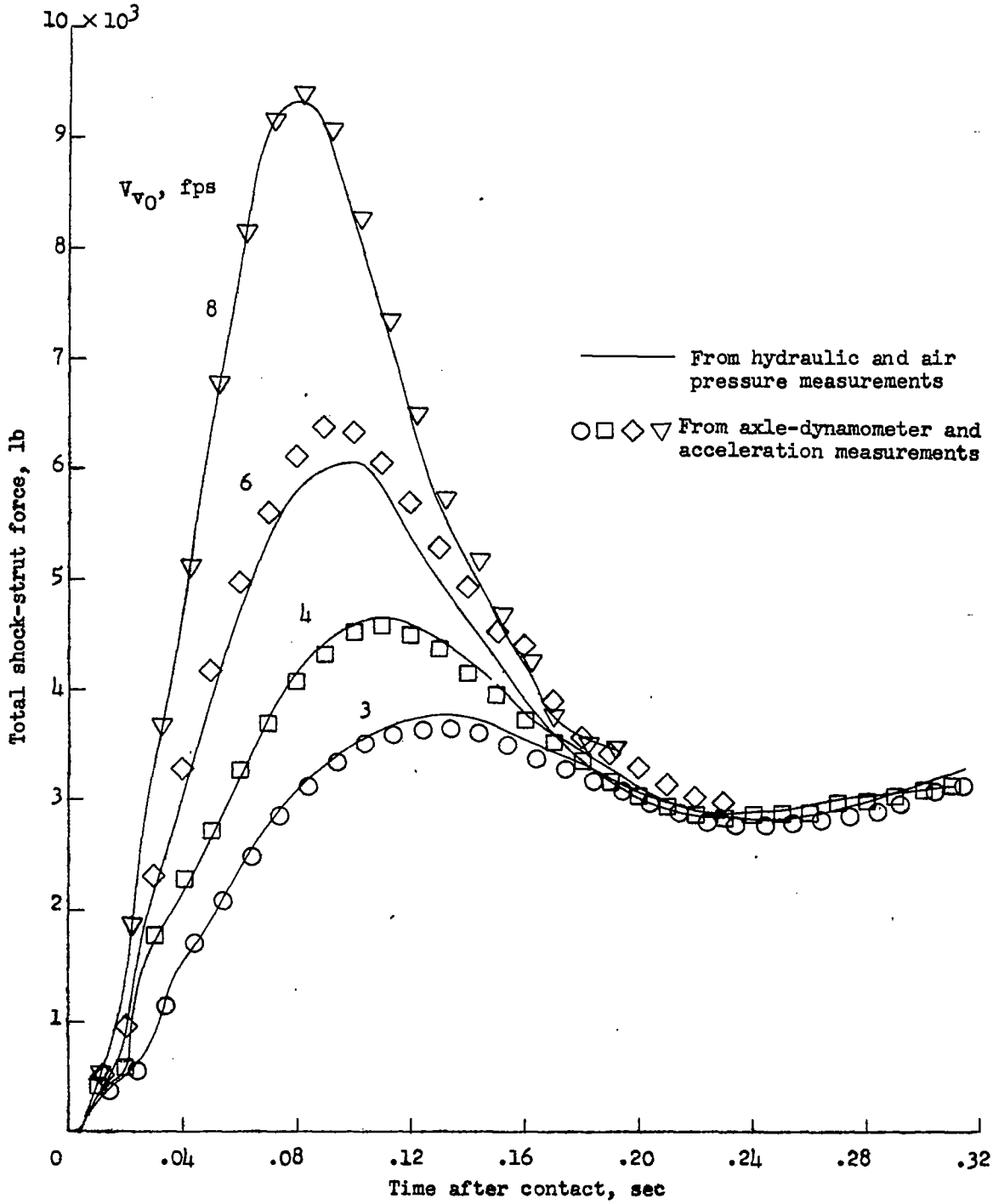

Figure 5.- Comparison between landing-gear load computed from pressure measurements and landing-gear load computed from dynamometer measurements.

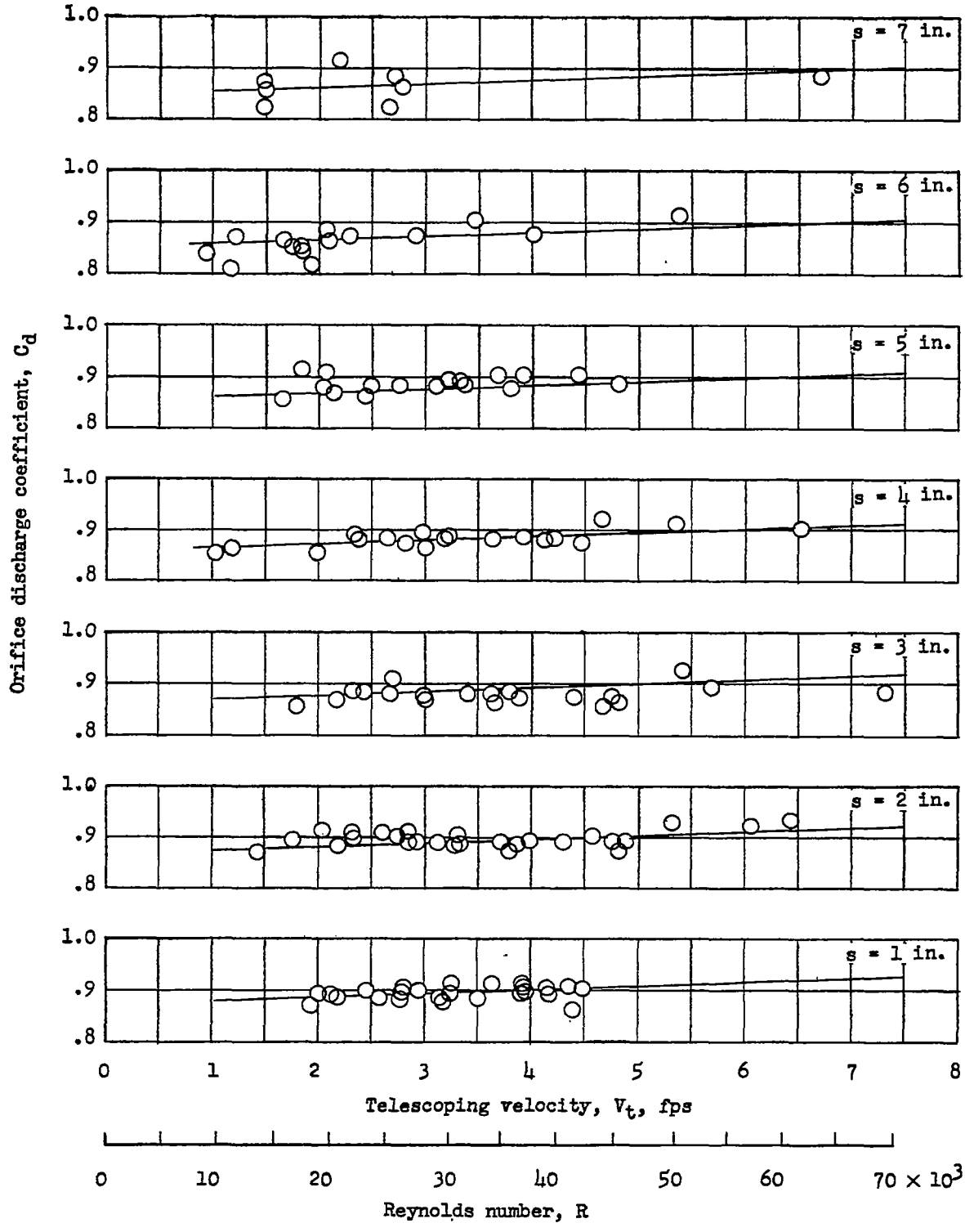

Figure 6.- Experimental variation of orifice coefficient with telescoping velocity or Reynolds number.

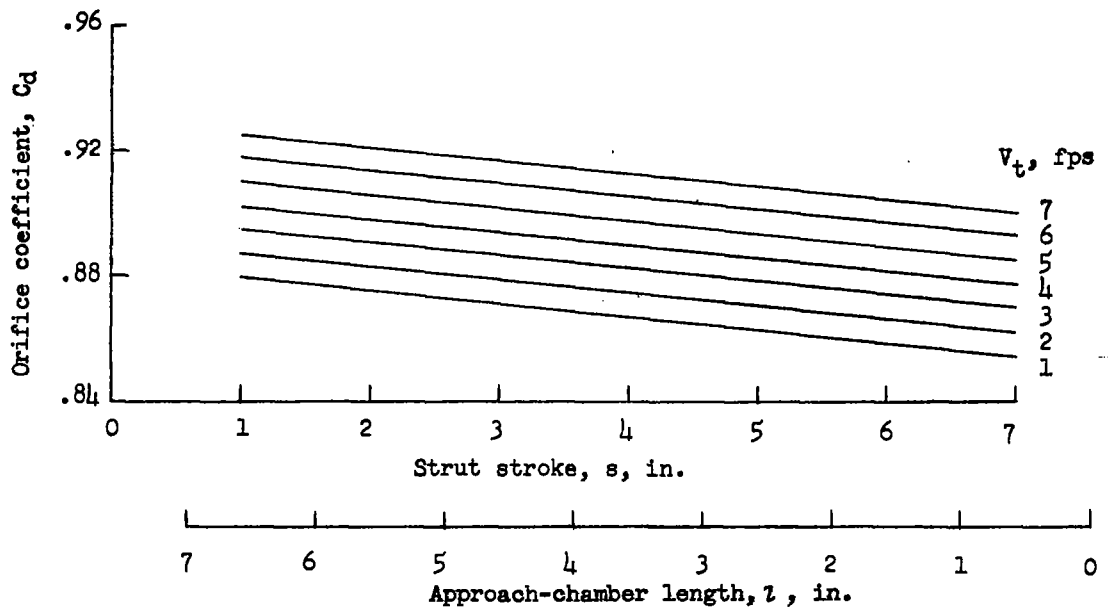

(a) Variation with strut stroke or approach-chamber length.

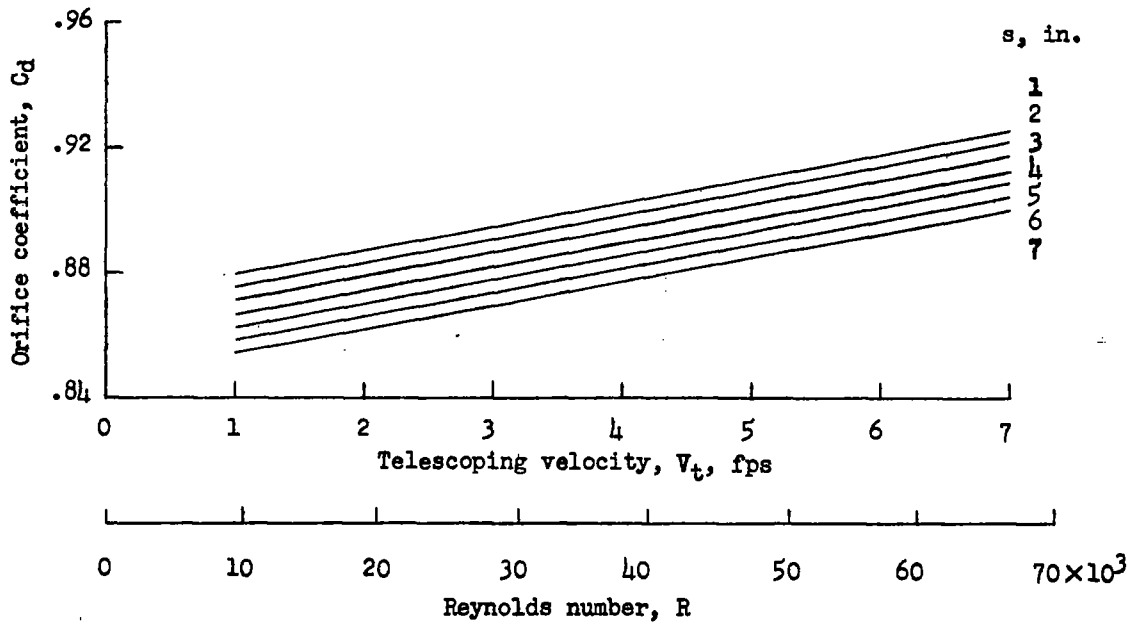

(b) Variation with telescoping velocity or Reynolds number.

Figure 7.- Experimental variation of orifice coefficient.

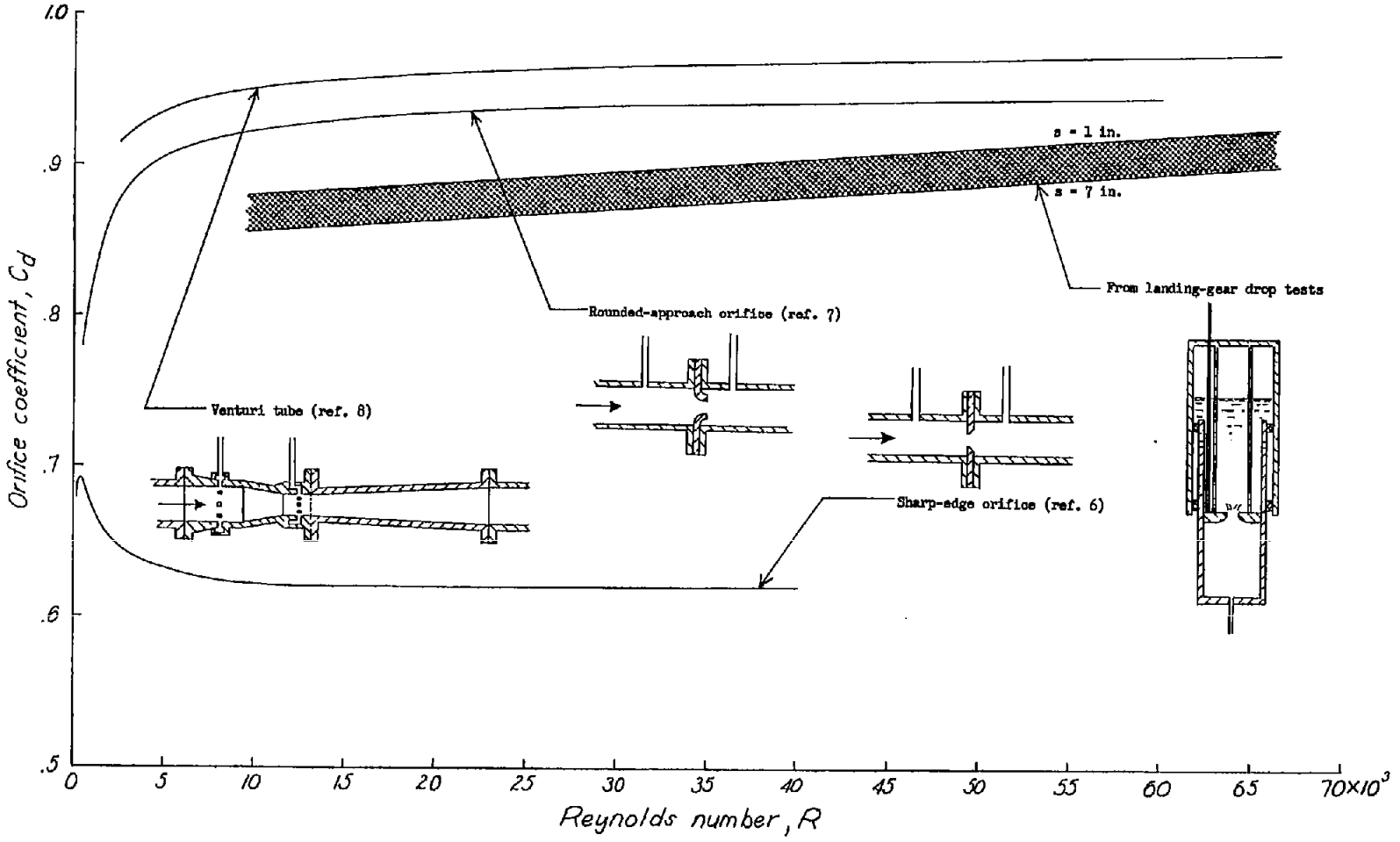

Figure 8.- Comparison of shock-absorber orifice coefficients with characteristic orifice-coefficient curves for three types of flow meters.

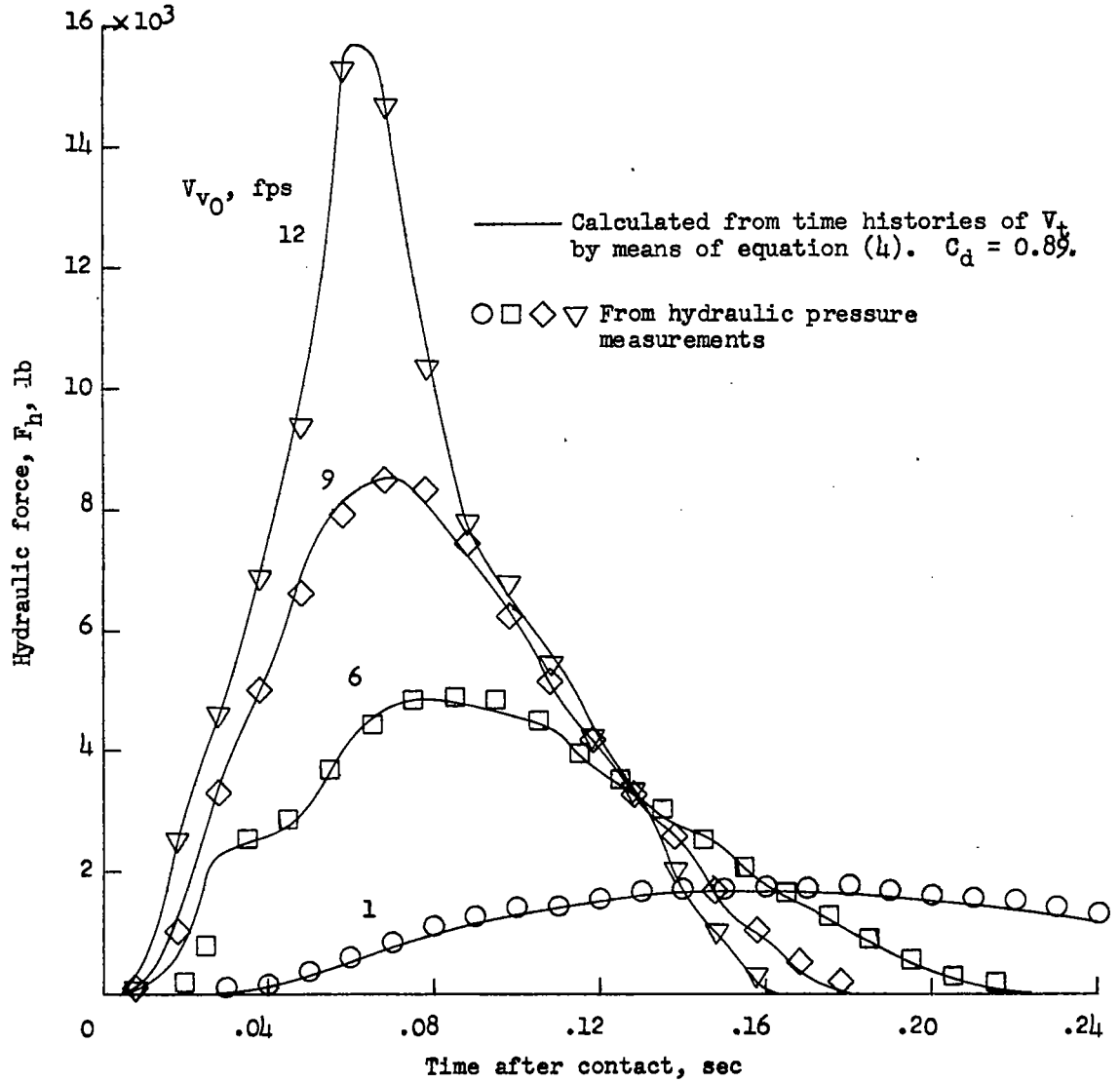

Figure 9.- Comparison between hydraulic-force time histories calculated from internal-pressure measurements and from measurements of telescoping velocity.

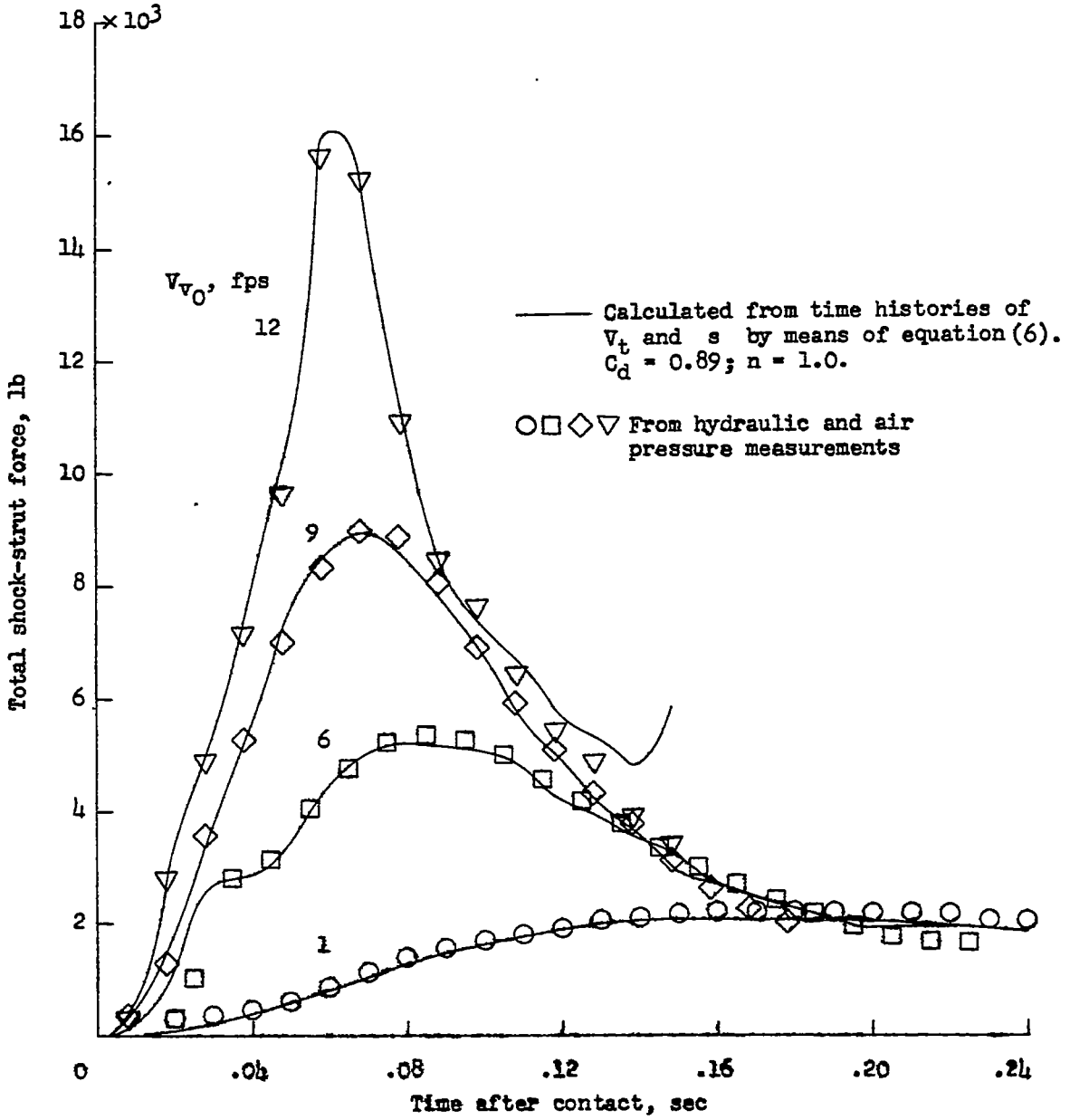

Figure 10.- Comparison between total-force time histories calculated from internal-pressure measurements and from measurements of telescoping velocity and strut stroke.

NACA-Langley - 4-5-55 - 1000